Carrier-Phase Multipath Calibration of GPS Reference Stations

LAMBERT WANNINGER
Ingenieurbüro Wanninger, Dresden, Germany

MANJA MAY
Department of Computer Science, Dresden University of Technology, Germany

Received September 2000; Revised July 2001

ABSTRACT: *Based on available GPS reference network observations, a procedure for estimating carrier-phase multipath corrections was developed, implemented, and tested. This procedure consists of three steps: detection and localization of multipath-affected satellite signals, daily estimation of multipath errors, and combination of these daily estimates to obtain corrections for undifferenced L_1 and L_2 phase measurements. After application of these corrections, multipath errors can be significantly reduced for frequently used linear combinations of dual-frequency observations, but not for the original L_1 and L_2 observations themselves. The reason lies in the relatively small multipath effects compared with the larger influence of remaining ionospheric errors in the multipath corrections. The variability of carrier-phase multipath errors over 1 year showed that on some days with snow cover, multipath errors were altered. No similar effects could be found on days with continuous rainfall.*

INTRODUCTION

Precise (centimeter-level) positioning requires the use of GPS carrier-phase observables. Regional reference station networks provide the opportunity to very precisely model and correct distance-dependent errors (ionospheric and tropospheric refraction, orbit errors; see, e.g., [1]). Therefore, carrier-phase multipath errors are the dominant error source for many applications, including real-time kinematic (RTK) and fast static positioning.

Multipath errors occur if the received signal is composed of the direct line-of-sight signal and one or more indirect signals reflected in the surroundings of the receiving antenna. The occurrence of multipath depends primarily on the reflectivity of the antenna environment. If the antenna is kept at the same position and the surroundings remain unchanged, multipath errors are merely a function of the azimuth and elevation of the satellites. Hence, multipath estimates can be extracted from previous observation data and then applied to correct current observations.

Recent advances in receiver technology have resulted in improved mitigation of code multipath. No such improvement, however, could be achieved for carrier-phase multipath, because its maximum effects occur even for very short excess signal paths (less than 1 m) for which essentially no mitigation is possible [2]. More important are methods based on an appropriate processing of the carrier-phase data. One such approach consists of multipath calibration of GPS reference stations.

The quality of carrier-phase multipath calibration is highly dependent on the ability to separate multipath effects from other errors. With closely spaced antennas, this requirement presents no difficulty, since carrier-phase multipath is the dominant error source. Furthermore, with antenna distances of several centimeters, multipath effects are highly correlated between antennas and can thus be estimated and eliminated [3, 4].

In the present approach, the GPS antennas are separated by several tens of kilometers, and thus each station has its own multipath characteristics. Moreover, distance-dependent error sources (especially ionospheric refraction, but also tropospheric refraction and orbit errors) dominate the error budget. These errors must be modeled and reduced first

doi: 10.1002/j.2161-4296.2001.tb00233.x

if multipath information is to be extracted from the GPS network observations.

The German networks of GPS reference stations consist of dual-frequency receivers with station distances of about 50 km. All stations are equipped with geodetic-type antennas. The observation data are available in RINEX format with time delays ranging from a few minutes to 24 h. The default epoch rate is 15 s. No signal-to-noise (S/N) values are provided with the observations.

The objective of the present study was to estimate carrier-phase multipath corrections for these reference stations exclusively from existing data. No additional GPS sites were established (not even temporarily). S/N values, which can provide valuable information for multipath detection and estimation, were not available [5].

A purely postprocessing software solution based on existing carrier-phase observations was developed. It provides multipath corrections that can then be applied to current observations in real time. The calibration procedure consists of three steps: detection and localization of multipath-affected satellite signals, daily estimation of multipath errors, and combination of these daily estimates to obtain corrections for undifferenced L_1 and L_2 phase measurements. The algorithm was implemented in the postprocessing software WaSoft of the Geodetic Institute, Dresden.

MULTIPATH EFFECTS ON LINEAR COMBINATIONS

The carrier-phase multipath error ε_M due to a single reflected signal component can be described as a function of the excess signal path (multipath delay), the ratio of direct signal amplitude to indirect signal amplitude (damping factor), and the carrier wavelength [6]:

$$\varepsilon_M = \frac{\lambda}{2\pi} \cdot \arctan \frac{\alpha \cdot \sin\left(\frac{d}{\lambda} \cdot 2\pi\right)}{1 + \alpha \cdot \cos\left(\frac{d}{\lambda} \cdot 2\pi\right)} \qquad (1)$$

where α is the damping factor, which varies between 0 and 1; d is multipath delay (m); and λ is carrier wavelength (m). Using the maximum value of the damping factor ($\alpha = 1$), the carrier-phase error can reach 0.25 λ, i.e., 4.7 cm and 6.1 cm for L_1 and L_2, respectively.

For precise relative positioning, linear combinations of the original phase measurements play an important role with regard to ambiguity resolution and coordinate estimation. These linear combinations are formed using

$$L_x = a_x \cdot L_1 + b_x \cdot L_2 \qquad (2)$$

where L_1, L_2 is the observable, residual or error of the original signal (m); a_x, b_x are coefficients; and L_x is the linear combination of observable, residual or error (m).

The widelane L_W with its coefficients

$$a_W = \frac{f_1}{f_1 - f_2} \text{ and } b_W = -\frac{f_2}{f_1 - f_2}$$

(f_1 and f_2 being the L_1 and L_2 signal frequency, respectively) is essential for fast and on-the-fly ambiguity resolution. The ionosphere-free linear combination L_0 with its coefficients

$$a_0 = \frac{f_1^2}{f_1^2 - f_2^2} \text{ and } b_0 = -\frac{f_2^2}{f_1^2 - f_2^2}$$

is used for coordinate estimation of baselines longer than 5 or 10 km to eliminate ionospheric effects. And the geometry-free (ionospheric) linear combination L_I with the coefficients $a_I = 1$ and $b_I = -1$ is often used for ambiguity resolution of short baselines with negligible ionospheric effects.

Forming these linear combinations, multipath effects are amplified. Simulated carrier-phase errors based on equations (1) and (2) and real multipath-contaminated double-differenced observations of a short baseline are presented in Figure 1. The sizes of the simulated and observed multipath effects agree very well. Maximum multipath errors increase by factors of 2 to 9 compared with their effects on the original carrier-phase observations.

Looking at the same real multipath errors but now for the double differences of a 30 km baseline, the difficulties of long-baseline multipath determination become visible (see Figure 1). Multipath is no longer the dominant error source. Relative ionospheric refraction effects caused by medium-scale variations in the ionospheric electron content can produce larger errors. Only the ionosphere-free linear combination shows variations in carrier-phase errors similar to those of the short baseline.

Medium-scale ionospheric disturbances, which are the most common form of ionospheric irregularities in midlatitudes, occur mainly during daylight hours in winter months in years of maximum solar activity [1]. They cause variations in relative positioning with periods ranging from 10 min to 1 h, and thus in the same frequency range as multipath effects. Separation of these two effects in the frequency domain is therefore impracticable. Unlike multipath, these relative ionospheric errors do not repeat and thus average out when one combines observations of several days. Nevertheless, the quality of multipath calibration in long baselines

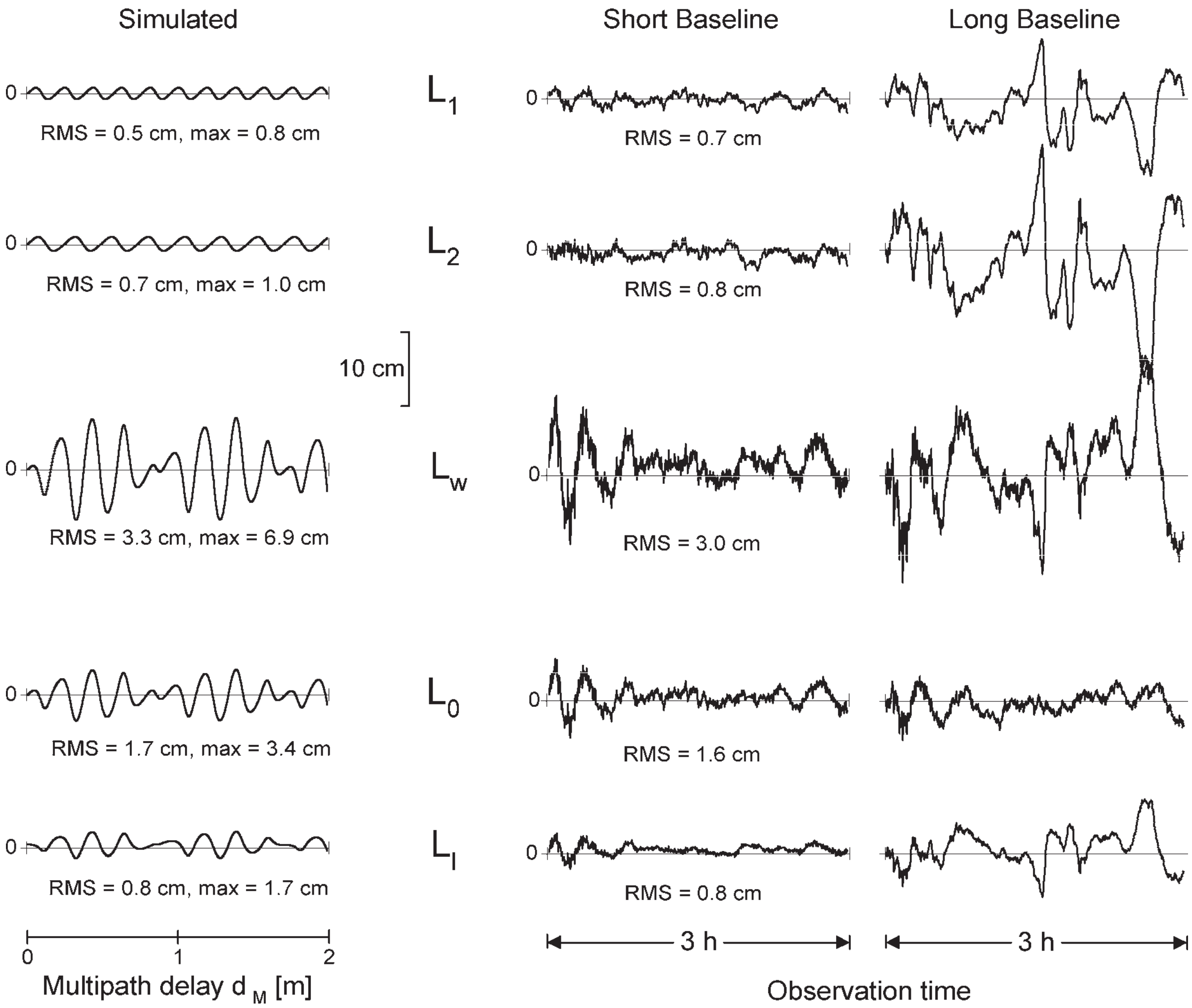

Fig. 1 – Simulated and Real Multipath Errors (The simulated errors ε_M are shown as a function of multipath delay and were computed for a damping factor α of 0.25. The real errors e_M of one GPS signal are shown in double-differenced residuals of a short baseline [1 km] and a long baseline [30 km]. In the long baseline, remaining ionospheric effects are the dominant error source.)

depends on the intensity of ionospheric disturbances.

GPS SATELLITE ORBITS

Multipath effects depend on the geometry of the satellites, the reflectors in the vicinity of the receiving antenna, and the position of the receiving antenna itself. Multipath effects can be expected to repeat with identical geometry of the satellite, the receiving antenna, and the signal reflectors.

As seen from any location on the earth's surface, GPS orbits repeat after about 1 sidereal day, i.e., 24 h minus 236 s. Therefore, multipath corrections can be stored as a function of satellite number and time to form multipath templates [7, 8].

In preparing the present correction model, the offset δ (s) of the time of two complete satellite revolutions from 1 mean solar day (= 86400 s) was estimated using

$$\delta = 86400 - \frac{4\pi}{n} \tag{3}$$

where n is corrected mean motion (rad/s), calculated from the GPS broadcast orbit parameters [9].

The satellite-specific variations of δ for the complete year of 1999 are shown in Figure 2. An average δ value of 245.6 s was found, which agrees well with the results of other research groups [10]. However, large outliers for two satellites that were moved within the GPS constellation were also detected. Commencing on day 30 of 1999, space vehicle (SV) pseudorandom number (PRN) 1 moved to a higher orbit and thus needed .5 min longer to complete two revolutions. SV8 was shifted to a lower orbit about day 275 and was thus 1.5 min per day faster than the other satellites.

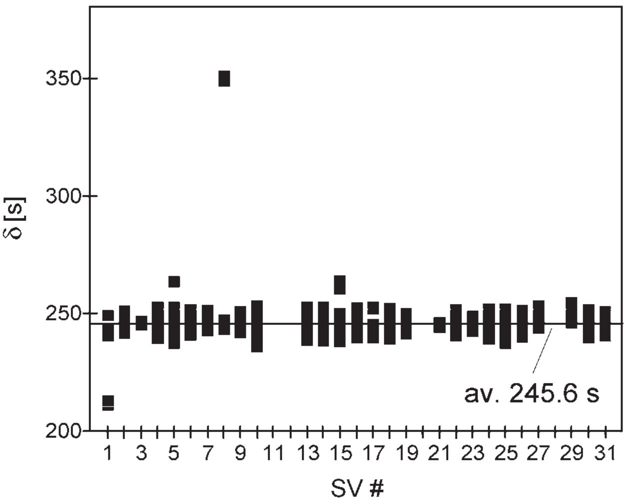

Fig. 2 – GPS Satellite Velocities for 1999 (shown as offsets δ of the time of two complete satellite revolutions from 1 mean solar day)

Another important consideration for longer-term multipath corrections is variations in the satellite orbits with respect to the observing station. All azimuth-elevation angles under which the satellites could be observed in 1999 were computed (see Figure 3). Corresponding to the satellite velocities of Figure 2, the variations in satellite orbits as seen from the receiving antenna are fairly small. The azimuthal variations at an elevation angle of 15 deg do not exceed 3 deg for most satellites. SV1 and SV8, however, encountered much larger variations. They scanned the sky with an azimuthal drift of up to 0.2 deg/day (SV1) or 0.5 deg/day (SV8). For these scanning satellites, multipath corrections have a very short effective lifetime of a few days. On the other hand, these satellites provide particularly useful information for a complete mapping of the multipath effects of a GPS reference station.

To be independent of these peculiarities of the GPS orbits, it was decided not to use multipath template techniques. Rather, multipath errors were considered to be a function of the direct signal incidence angle, and thus multipath corrections were mapped in a coordinate system of azimuth and elevation.

DETECTION AND LOCALIZATION OF CARRIER-PHASE MULTIPATH

Multipath effects can be detected in time series of double-differenced residuals of the carrier-phase observables. The ionosphere-free linear combination is especially suitable for multipath detection since it is much more affected by multipath than the original signals (see Figure 1). Furthermore, detection can be performed even for baselines longer than a few kilometers because of the elimination of ionospheric refraction effects.

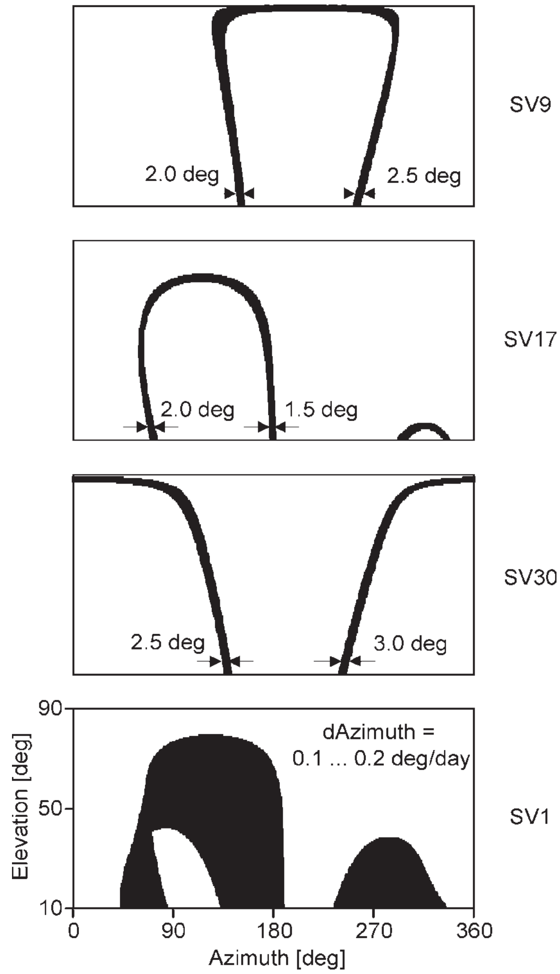

Fig. 3 – Azimuth-Elevation Coverage of Selected GPS Satellites for a Central European Station, 1999

The detection algorithm is based on the following characteristics of multipath effects:

- The dominant multipath periods range from 10 to 45 min, depending mainly on the reflector-antenna distance. Since ionospheric refraction has been eliminated by forming the ionosphere-free linear combinations, no other error source with a similar characteristic remains.
- Because the GPS antennas are located on rooftops, all reflectors are situated below the antenna horizon. Thus satellite signals incident from low elevations (e.g., below 50 deg) are expected to be affected, and signals coming from higher elevations (e.g., above 50 deg) are expected to show little effect.
- Multipath effects are uncorrelated between reference stations since each roof and antenna position has its individual characteristics.

The detection and localization algorithm consists of the following steps:

- Compute undifferenced residuals of the ionosphere-free linear combination (similar to producing carrier-phase corrections according to [11]).

- Form 20 min blocks of low-elevation data (below 50 deg), and test them individually using the following three steps:
  - Form double-differenced residuals from undifferenced data using the observations to be tested, simultaneous observations of the highest elevated satellite at the same station, and the corresponding observations at the other stations in the network. This step results in (n − 1) vectors of double-differenced observations in a network of n stations (see Figure 4).
  - Reduce each vector by the average value of all its elements to remove the carrier-phase ambiguities, the remaining tropospheric effects, and the influence of orbit errors. If the standard deviations of the majority of vectors exceed a predefined limit (e.g., 15 mm), multipath can be suspected (see Table 1).
  - Correlate the vectors of double-differenced observations in all combinations. If the majority of correlation coefficients exceeds a predefined limit (e.g., 0.8) the detected multipath effects are caused by the undifferenced observations to be tested (see Table 1).

Note that this algorithm does not require any ambiguity fixing to integer values. Nor does the algorithm produce any better results if the broadcast ephemerides are replaced by precise ephemerides.

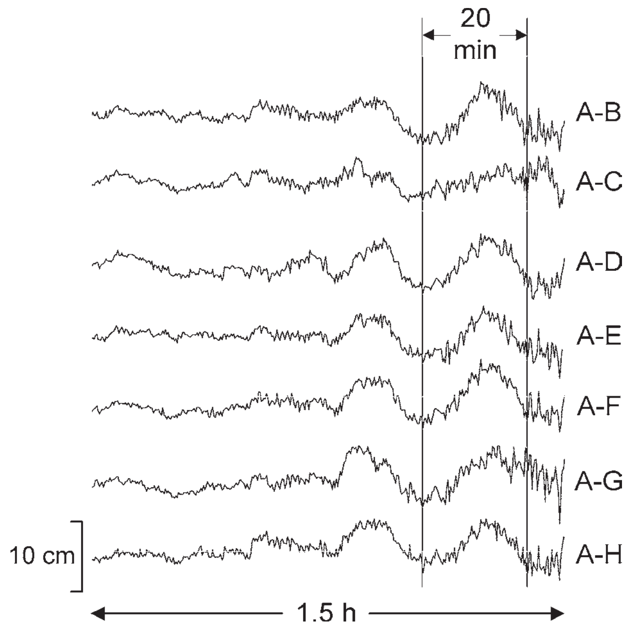

Fig. 4 – Ionosphere-Free Double-Differenced Residuals for a Satellite Below 50 deg of Elevation Observed from Station A (These residuals were formed using the observations of a satellite above 50 deg elevation, assumed to be multipath-free, and the corresponding observations at stations B to H.)

Table 1 – Standard Deviations and Correlation Coefficients for 20 min Time Period Indicated in Figure 4

Baseline	Std. Dev. (mm)	Correlation Coefficients A-C	A-D	A-E	A-F	A-G	A-H
A-B	31	.66	.95	.94	.96	.80	.95
A-C	14	—	.73	.67	.70	.73	.67
A-D	27	—	—	.94	.97	.82	.94
A-E	26	—	—	—	.93	.80	.93
A-F	30	—	—	—	—	.83	.95
A-G	27	—	—	—	—	—	.78
A-H	23	—	—	—	—	—	—

An example of multipath detection and localization is presented in Figure 4 and Table 1. A 20 min block of observations of the signal of a specific satellite observed from station A is tested against the observations of seven other stations in the network. The standard deviations of the seven double-difference vectors exceed 15 mm with one exception (baseline A-C). Sixty-seven percent of the correlation coefficients are larger than 0.8. Thus multipath effects were detected, and the responsible undifferenced observations (satellite, station) could be identified.

The smaller standard deviation and correlation coefficients for baseline A-C are caused by multipath effects for the same satellite but at station C. The multipath effects at A and at C for this satellite and in this period of 20 min are highly similar, and thus they largely cancel out in the double differences, which results in a small standard deviation.

The example shows that this detection and localization algorithm requires a majority of unaffected signals to be able to identify the affected ones. Fortunately, the strongly affected stations within the German reference networks comprise only about 20 percent of all stations [12].

Furthermore, the detection and localization procedure can be subdivided. In a first step, all stations of a network are processed simultaneously to separate severely affected from slightly affected stations. In the second step, the slightly affected stations are processed separately, and each severely affected station is tested against the group of slightly affected stations.

Experience with this detection and localization algorithm has shown that in reference station networks with station separations of some 50 km, reliable results can already be obtained with single 24 h datasets (60 s data rate). To verify the results, the procedure is usually repeated with a second 24 h dataset. In general, the differences between two independent detections are negligible.

Having identified a multipath-affected portion of a signal, the azimuth and elevation of the transmitting satellite are stored in a grid format with a rectangular resolution of 2 deg (elevation) $\times$ 10 deg (azimuth). For each bin, an average standard deviation value based on the double-difference standard deviations is produced to provide an indication of the intensity of the multipath errors.

The test network consists of nine stations owned by the State Survey Department of Sachsen-Anhalt, Germany. The multipath detection algorithm was applied to the network observation data for 1999. Since no considerable day-to-day variations of detected multipath could be observed, the daily detection grid maps were combined to form station maps (see Figure 5).

Five stations can be considered as (almost) multipath-free (BITT, LOBU, LUW2, SAN2, WEI2); some multipath effects could be detected for two stations (HALW, STAF); and the signals of the remaining two stations were severely affected (DESS, MAGD). This finding agrees with earlier results indicating that about 20 percent of the German reference stations suffer from severe carrier-phase multipath effects. A majority of stations are (almost) multipath-free and can thus be used to determine multipath corrections for the severely affected stations.

CARRIER-PHASE MULTIPATH CALIBRATION

To be able to determine carrier-phase multipath corrections, ambiguity resolution is required for all baselines of the network. Since the coordinates of the reference stations are known precisely and data processing can be performed in postprocessing, ambiguity resolution presents no real difficulty.

The carrier-phase observations are stored and handled in undifferenced mode. Compared with a single-difference approach, the present method has the advantage that after ambiguity resolution, the observations of all stations and satellites are on the same ambiguity level. That is, ambiguity-free double-differenced observables between any stations and satellites can easily be formed.

For both ambiguity resolution and multipath correction, an attempt is made to keep the effects of distance-dependent errors as small as possible. From the geometry-free linear combination of the carrier-phase data, a single-layer model of the vertical ionospheric electron content (VEC) in a coordinate system of geographic latitude φ and local time t is estimated (cf. [13]):

$$\mathrm{VEC}(\varphi, t) = a_{00} + a_{10} \cdot (\varphi - \varphi_0) + a_{01} \cdot (t - t_0) + a_{02} \cdot (t - t_0)^2 \quad (4)$$

where a_{ij} is the model coefficients, and φ_0, t_0 are the coordinates of the selected origin of a local coordinate system. This model yields the observations equation of the geometry-free (ionospheric) linear combinations of carrier-phase data:

$$L_I = m_I \cdot \mathrm{VEC}(\varphi, t) + C_I^i \quad (5)$$

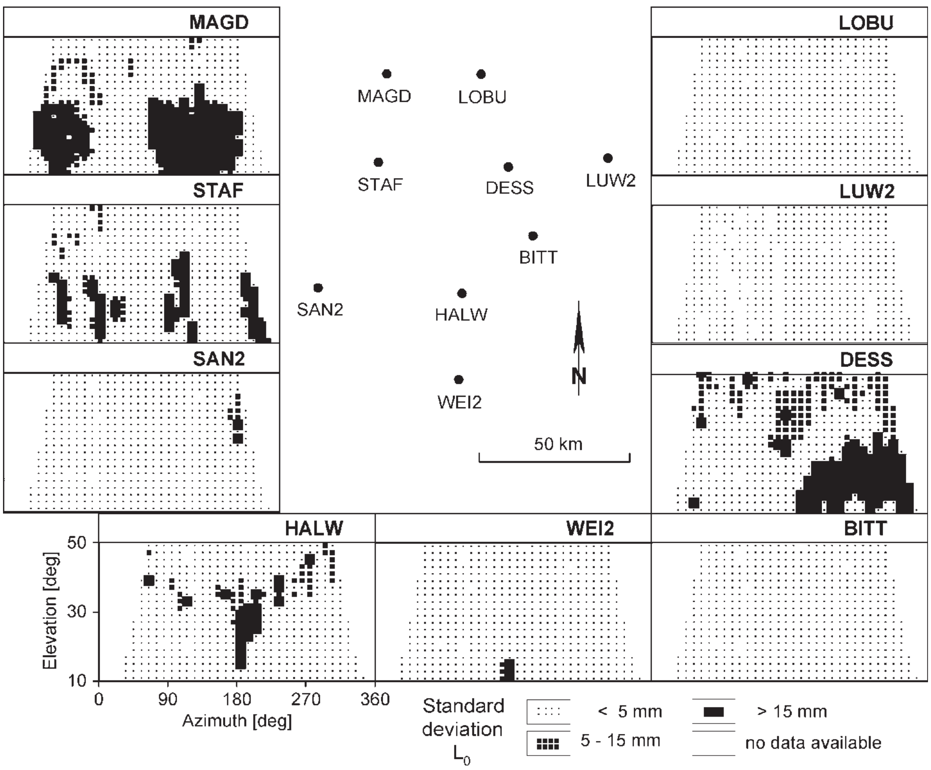

Fig. 5 – GPS Reference Station Network Consisting of Nine Stations: Multipath Detection Results for Each Station

Equation (5) contains the ionospheric mapping function m_I, the VEC at the intersection of the signal path and the ionospheric layer, and satellite-individual constants C_I that absorb the undifferenced carrier-phase ambiguities and differential hardware delays.

Sets of the VEC model coefficients are estimated by least-squares adjustment for observation times of 3 h, and the ionospheric corrections are applied to the undifferenced L_1 and L_2 observations. With these models, it is possible to reduce considerably the effects of large-scale features of the ionosphere. It is not possible, however, to remove the effects of medium-scale ionospheric features, which represent the main error source in multipath calibration in regional GPS networks.

Tropospheric corrections are applied according to a standard atmospheric model. Additionally, residual zenith delays are calculated from the GPS network data. One zenith delay parameter per station is estimated for each 4 h of observations. The estimated tropospheric corrections are then applied to the undifferenced L_1 and L_2 observations.

The introduction of precise International GPS Service (IGS) orbits had essentially no effect on the ambiguity resolution, nor did it noticeably improve the estimated multipath corrections. Hence, only the GPS broadcast orbits were used.

After ambiguity resolution and mitigation of the distance-dependent error, multipath corrections are estimated for each L_1 and L_2 observation separately according to the following double-difference algorithm. Multipath estimations are performed only for those selected stations S and selected satellites s for which multipath errors were detected with L_0 standard deviations larger than 15 mm (cf. Figure 5). Reference satellites j are all those satellites with elevations larger 50 deg. It is assumed that their signals are not affected by multipath. All those stations with no detected multipath (L_0 standard deviation below 5 mm) for satellites s serve as reference stations I. Multipath estimates e_M are then obtained from

$$e_M = \frac{1}{\Sigma_W} \cdot \sum_{I=1}^{N} \sum_{j=1}^{m} (r_S^s - r_S^j - r_I^s + r_I^j) \cdot w_{SI} \quad (6)$$

where r is undifferenced L_1 or L_2 carrier-phase residuals with double-differenced ambiguities resolved and ionospheric and tropospheric correction applied as described above, and a weighting factor $w_{SI} = 1/d_{SI}$ is applied as a function of the distance d_{SI} between the selected station S and the reference station I. The multipath estimates are stored together with an identifier for station S, azimuth and elevation of satellite s, and time.

In a subsequent step, multipath corrections were estimated over a grid. Several pixel sizes were tested, ranging from 0.1×0.1 deg to 1×1 deg in azimuth and elevation. Since it was not possible to detect improved multipath corrections with higher resolution, the most storage-efficient resolution of 1×1 deg was used. Basically, all multipath estimates that fell into the same pixels were averaged. A two-step approach made it possible to detect outliers and remove them from further data processing. Calibration maps can now be produced on the basis of multipath estimates ranging in scope from a single day to several days or even a whole year.

1999 CALIBRATION RESULTS

The multipath detection within the test network revealed that two of nine reference stations show some multipath effects, and another two are severely affected by carrier-phase multipath (cf. Figure 5). The calibration algorithm described above was applied to all affected stations, but the presentation of results here is limited to the most-affected stations, DESS and MAGD.

To present a complete picture of multipath corrections, multipath estimates e_M were calculated not just for those 2×10 deg detection pixels with L_0 standard deviations larger 15 mm, but for all observations below 50 deg elevation angle. Using the observations of the entire year of 1999 and averaging the estimates e_M within each 1×1 deg calibration pixel yields L_1 and L_2 calibration maps (see Figure 7). The corresponding calibration maps for linear combinations were calculated using equation (2).

No calibration values can be obtained for northern directions because no GPS satellite signals are received from this part of the sky. Some smaller gaps can be observed around 90 and 200 deg of azimuth where no signals were incident in 1999. These remaining gaps are fairly small because of the scanning satellites SV1 and SV8. Multipath correction values were obtained for 69 percent of all 1×1 deg pixels between 10 and 50 deg of elevation. Without the two scanning satellites, the percentage would have been only 23. This, however, is not a drawback to multipath calibration because no corrections are needed for those incident angles without satellite signals.

The GPS antennas at both stations DESS and MAGD are mounted on roofs. No obstructions or reflectors exist above the antenna horizons (see Figure 6). Hence, only the roofs themselves need be considered potential reflectors.

In the case of DESS, the roof right below the antenna (the upper roof in Figure 6) expands from 170 deg in azimuth to the northern direction. Within this azimuth range and for elevations below 30 deg, large multipath corrections were determined (see

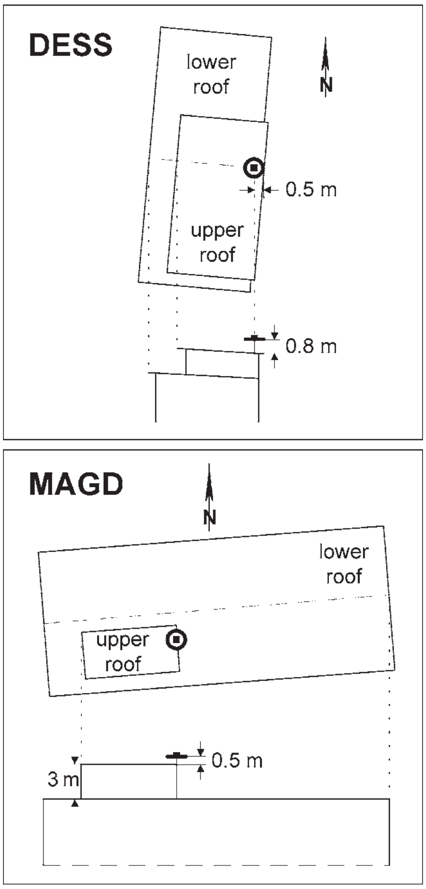

Fig. 6 – Surroundings of the GPS Reference Antennas at Stations DESS and MAGD

Figure 7). The wavelike pattern of these corrections with a wavelength of about 7 deg in elevation indicates that the reflector is located very close to the antenna. Since the roof is tilted to the eastern direction, the multipath waves are bent with an elevation maximum at about 270 deg in azimuth.

At DESS, no significant multipath corrections were obtained for signals from low-elevation satellites within the azimuth range of 30 to 160 deg. This result agrees quite well with the multipath detection results (cf. Figure 5) and can easily be explained by the antenna surroundings. Because the antenna is mounted close to the eastern edge of the roof, no reflectors exist for signals incident from low elevations. The signals coming from elevations above 40 deg, however, are affected by multipath, which can originate only from the small roof strip between the antenna and roof edge. Multipath was already apparent in the detection results (see Figure 5).

At MAGD, two reflector surfaces exist: a lower roof at a distance of a few meters and an upper roof right below the antenna (see Figure 6). Since both surfaces are flat, i.e., not tilted, the multipath patterns are constant for constant elevations. The wavelengths of the multipath patterns in elevation amount to about 7 deg for the upper roof (azimuth range from 160 to 280 deg) and about 2.5 deg for the lower roof (from 0 to 160 deg).

Looking at the calibration maps of different linear combinations, earlier findings are confirmed that in the original L_1 and L_2 observations, multipath signals have small amplitudes and are thus difficult to detect. Other linear combinations, such as the widelane L_W, the ionosphere-free signal L_0, and even the geometry-free signal L_I, are much more affected.

DAY-TO-DAY VARIABILITY OF MULTIPATH EFFECTS

An important aspect of multipath calibration is the variability of carrier-phase multipath effects with environmental changes in the antenna vicinity. In the present case, typical changes may be caused by rain and snow, which are expected to affect the reflectivity of the roof surfaces.

To test the validity of multipath corrections, L_1 and L_2 calibration maps were produced for DESS from all the 1999 data. In contrast with Figure 7, correction values were now determined only for pixels with a detected multipath strength of more than 15 mm L_0 standard deviation (cf. Figure 5).

Daily solutions for the baseline DESS-BITT (24 km) were determined with the original DESS observations, as well as with multipath-corrected observations. The least-squares adjustment provides the standard deviation of the observables as an indicator for the size of observation errors. Comparing these indicators of the daily solutions with and without multipath corrections shows how effectively multipath correction works for this 24 km baseline. Negative percentage values in Figure 8 indicate mitigation of multipath effects. The average improvement is very small for L_1 and L_2 (less than 1 percent) but reaches significant values for the three linear combinations L_W, L_0, and L_I.

Note that multipath corrections were applied to only 9 percent of all DESS observations, i.e., those most affected. Correction of all observations within an elevation range of 10 to 50 deg (70 percent of all observations) further reduces the errors in L_0 and L_W, but significantly degrades the L_1 and L_2 solutions because of the introduction of additional ionospheric errors.

Looking at the day-to-day variability of the reduction in observation error, one notes a seasonal variation in all signals that are affected by the ionosphere, i.e., in all signals except L_0. This effect can be explained by the influence of medium-scale ionospheric disturbances, which occur mainly in the winter. Because of the larger relative ionospheric errors at the beginning and end of 1999, multipath is responsible for a smaller portion of the overall

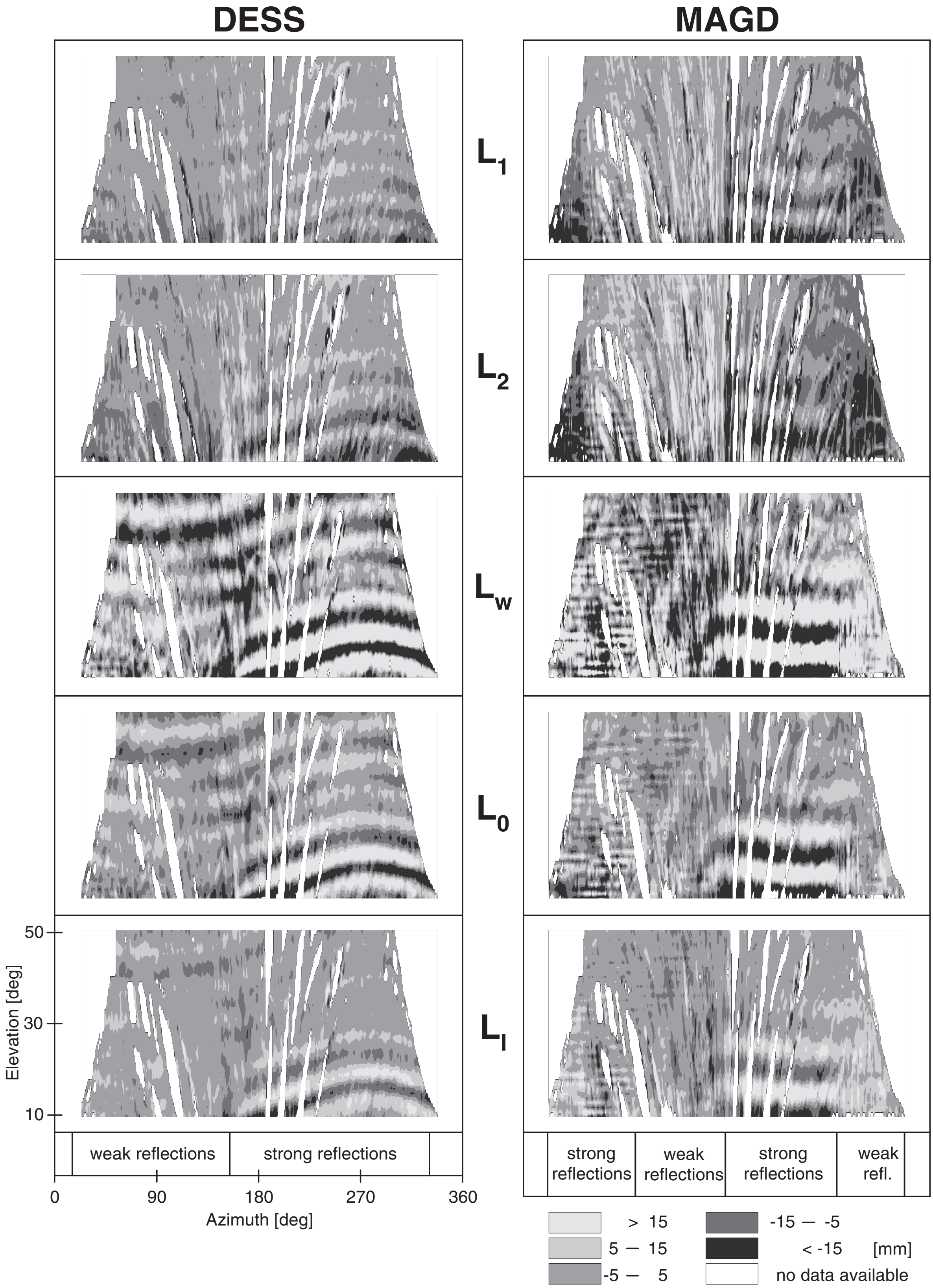

Fig. 7 – 1999 Calibration Results for DESS and MAGD

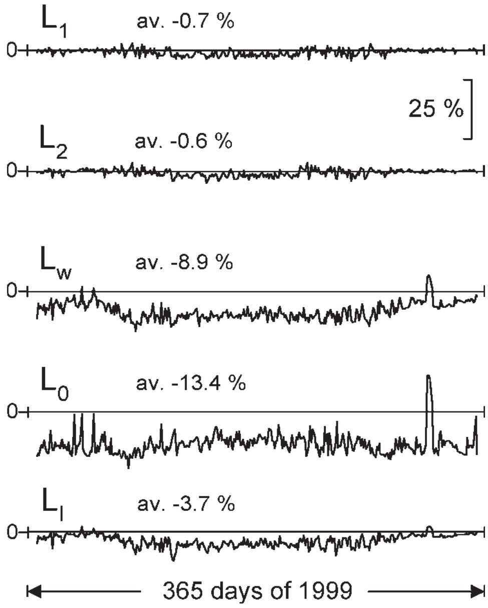

Fig. 8 – Effect of Multipath Corrections on Overall Observation Errors in the 24 km Baseline DESS-BITT (Negative values indicate a reduction in observation errors due to multipath corrections.)

error budget, and thus multipath mitigation has smaller effects.

Some outliers can be detected, especially in the ionosphere-free linear combination L_0 on days 32, 38, 48, 324–328, and 364. Upon checking the weather records for that area, it was found that on 6 of these 8 days, temperatures were below 0°C, and snowfall was reported. Unfortunately, it was not possible to verify precisely whether the roof or the antenna was covered with snow. Nevertheless, there are strong indications that these outliers were caused by snow. No similar conclusion can be drawn for variations due to rainfall and thus the wetness of the reflectors. Continuous rainfall was reported for 23 days, but no effects can be found in the multipath mitigation results.

APPLICATION OF MULTIPATH CORRECTIONS TO FURTHER TEST DATA

A further test dataset was observed at the end of May 2000. In the direct vicinity of the reference station DESS, three GPS receivers were employed at stations nearly free of any multipath effects, and 24 h of observations was collected. The objective was to test the effectiveness of multipath corrections obtained from a regional network of GPS reference stations and applied to short baselines.

Double-differenced carrier-phase residuals of the short baselines (1 km) to DESS served as the multipath indicator. Since no distance-dependent error sources can produce significant errors on these short baselines, multipath is the dominant error source for all signals. Comparing double-differenced residuals before and after multipath correction of the observations collected at DESS provides a good estimate of the extent of multipath mitigation.

A representative example of double-differenced residuals is presented in Figure 9. The original data clearly show oscillating multipath errors that disappear after the application of multipath corrections. Root-mean-square (RMS) values of double-differenced residuals are reduced by 30 to 50 percent for widelane L_W, ionosphere-free L_0, and geometry-free L_I linear combinations. The original L_1 and L_2 observations, however, show no improvement, and even worse, double-differenced residuals in L_2 are amplified.

Averaged standard deviations for all baselines from the three local stations to DESS provide similar results. Here, several kinds of correction models were also tested; the results of three of these models are presented in Table 2. The objective was to

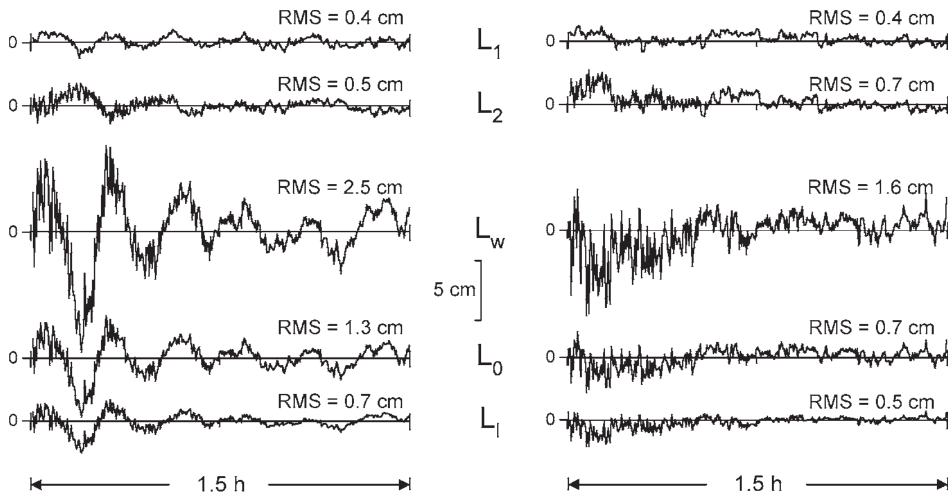

Fig. 9 – Mitigation of Multipath Effects in a Short Baseline (Shown are double-differenced residuals and RMS values before [left] and after [right] multipath correction.)

Table 2 – Short-Baseline (1 km) Standard Deviations of Observation Residuals (mm)

	L_1	L_2	L_W	L_0	L_I
Uncorrected	3.5	5.0	20.2	10.0	5.3
Corrected with Model					
Based on Data of					
Previous day	5.0	7.1	17.7	8.9	4.9
Previous 10 days	3.5	5.1	17.2	8.5	4.6
Year 1999	3.9	5.8	17.0	8.3	4.7

determine how many days of multipath estimates is needed to produce a good calibration result. Hence, corrections from an increasing number of previous days were estimated.

With a single previous day, improvements are already seen in the linear combinations, but ionospheric errors deteriorate the L_1 and L_2 results. With 10 days of multipath estimates, L_1 and L_2 standard deviations are as large as those without corrections, but significant improvements can be achieved in the linear combinations. No further improvements can be achieved using multipath estimates of more than 10 previous days. Applying the 1999 calibration model to the May 2000 data produces results almost as good as those derived with multipath estimates of the previous days. Unfortunately, L_1 and L_2 observations deteriorate again.

The same tests were performed for a 24 h sample of the 24 km–long baseline DESS-BITT (see Table 3). Here, remaining ionospheric refraction is the dominant error source for all signals except the ionosphere-free linear combination L_0. The model based on the multipath estimates of 10 previous days produces the best results. The corrections from 1999 are of similar quality.

The test results show that it is possible to considerably reduce observation errors in the linear combinations L_W, L_0, and L_I for reference stations affected by large multipath errors. On the other hand, no improvements can be achieved for L_1 and L_2. The calibration algorithm must be carefully tuned so that no additional (ionospheric) errors are introduced into the L_1 and L_2 observables.

Table 3 – Long-Baseline (24 km) Standard Deviations of Observation Residuals (mm)

	L_1	L_2	L_W	L_0	L_I
Uncorrected	21.9	34.8	33.3	11.7	26.9
Corrected with Model					
Based on Data of					
Previous day	22.4	35.4	31.9	10.9	26.6
Previous 10 days	22.0	34.9	31.6	10.7	26.4
Year 1999	22.1	35.0	31.5	10.6	26.4

CONCLUSION

Carrier-phase multipath corrections were extracted from the observations of a regional GPS network. The calibration algorithm consists of three distinct steps: detection, localization, and calibration of carrier-phase multipath. The corrections are applied to the undifferenced observations of the reference stations.

Observation of carrier-phase multipath over 1 year revealed large variations on days with snow cover on the reflectors (or possibly on the antenna). No such variations could be attributed to rainfall and thus the wetness of the reflectors.

Multipath errors could be reduced significantly in widelane L_W, ionosphere-free L_0, and geometry-free L_I linear combinations. No such improvements could be achieved for the L_1 and L_2 signals because multipath has a much smaller effect on these signals than on linear combinations based on them. In L_1 and L_2, remaining ionospheric errors in the multipath correction models canceled any improvements due to multipath mitigation.

It can be expected that the shorter the station distances in the reference station network, the better will be the multipath mitigation results using the described algorithm.

ACKNOWLEDGMENTS

The GPS reference station observations were made available by the State Survey Department of Sachsen-Anhalt, Halle, Germany. The work described in this paper was performed while both authors were with the Geodetic Institute, Dresden University of Technology, Germany.

Based on a paper presented at The Institute of Navigation ION GPS-2000, Salt Lake City, Utah, September 2000.

REFERENCES

1. Wanninger, L., *The Performance of Virtual Reference Stations in Active Geodetic GPS-Networks Under Solar Maximum Conditions*, Proceedings of ION GPS-99, September 1999, pp. 1419–27.
2. Weill, L. R., *Conquering Multipath: The GPS Accuracy Battle*, GPS World, April 1997, pp. 59–66.
3. Brown, A. and J. Wang, *High Accuracy Kinematic GPS Performance Using a Digital Beam-Steering Array*, Proceedings of ION GPS-99, September 1999, pp. 1685–93.
4. Ray, J. K., *Use of Multiple Antennas to Mitigate Carrier Phase Multipath in Reference Stations*, Proceedings of ION GPS-99, September 1999, pp. 269–79.
5. Axelrad, P., C. Comp, and P. MacDoran, *Use of Signal-to-Noise Ratio for Multipath Error Correction in GPS Differential Phase Measurements: Methodology and Experimental Results*, Proceedings of ION GPS-94, September 1994, pp. 655–66.

6. Georgiadou, Y. and A. Kleusberg, *On Carrier Signal Multipath Effects in Relative GPS Positioning*, Manuscripta Geodaetica, 13, 1988, pp. 172–79.
7. Bishop, G. J. et al., *Studies and Performance of a New Technique for Mitigation of Pseudorange Multipath Effects in GPS Ground Stations*, Proceedings of The Institute of Navigation's National Technical Meeting, January 1994, pp. 231–42.
8. Kee, C. and B. Parkinson, *Calibration of Multipath Errors on GPS Pseudorange Measurements*, Proceedings of ION GPS-94, September 1994, pp. 353–62.
9. *Interface Control Document: NAVSTAR GPS Space Segment / Navigation User Interfaces* (ICD-GPS-200), ARINC Research Corporation, El Segundo, CA, 1997.
10. Seeber, G. et al., *Precise GPS Positioning Improvements by Reducing Antenna and Site Dependent Effects*, IAG Proceedings, Vol. 118, 1997, pp. 237–44.
11. *RTCM Recommended Standards for Differential GNSS Service*, Version 2.2, RTCM Paper 11-98/ SC 104-STD, Alexandria VA, 1998.
12. Wanninger, L. and S. Wildt, *Identifikation von Mehrwegeeinflüssen in GPS-Referenzstationsbeobachtungen*, Allgemeine Vermessungs-Nachrichten (AVN), 104, 1997, pp. 12–15.
13. Georgiadou, Y. and A. Kleusberg, *On the Effect of Ionospheric Delay on Geodetic Relative GPS Positioning*, Manuscripta Geodetica, 13, 1988, pp. 1–8.